

# A 120-330V, sub- $\mu$ A, 4-Channel Driver for Microrobotic Actuators with Wireless-Optical Power Delivery and over 99% Current Efficiency

Jan S. Rentmeister<sup>1</sup>, M. Hassan Kiani<sup>1</sup>, Kristofer Pister<sup>2</sup>, and Jason T. Stauth<sup>1</sup>

<sup>1</sup>Thayer School of Engineering at Dartmouth, Hanover, NH; <sup>2</sup>University of California, Berkeley, CA

## Abstract

This work presents a 4-channel, mm-scale, electrostatic and piezoelectric actuator driver that uses  $< 1\mu\text{A}$  total quiescent bias current and can drive actuator loads up to 120-330V at frequencies over 1kHz. The driver achieves over 99% current efficiency and can operate untethered with an integrated photovoltaic array driven by a collimated or diffuse optical power source. The circuit is tested with an off-chip boost circuit, generating over 1.5kV with 85% power efficiency at 45mW load. The system uses a simple 4-bit CMOS logic level interface with 100 kHz clock to actuate high voltage channels; on-chip photovoltaics also power the digital controller, and I/O bus. **Keywords:** MEMS, DC-DC Converter, micro-robotics.

## Introduction

Micro- and mm-scale robotic integration is promising for a variety of applications, but requires high-voltage electronics to actuate piezo- or electrostatic mechanical transducers [1]. Such electronics is ideally small, lightweight, and capable of driving multiple channels while untethered from physical wires [2]. Voltage requirements range from 30V-3kV at frequencies of 10-100's of Hz with actuators presenting as dominant-capacitive loads (10pF-10nF). Optical wireless power delivery can provide 100's of  $\mu\text{W}/\text{mm}^2$  without the strict range limitations of near-field (inductive) coupling, yet remains underexplored for robotic applications.

## Design Overview

This work presents a multi-channel actuator driver in a 650V SOI CMOS process, powered wirelessly by an on-chip silicon photovoltaic (PV) array, excited with a collimated (laser) or diffuse light source, or optionally by an off-chip voltage source. Shown in Fig. 1, the system comprises 4 actuation channels, each capable of driving a reactive actuator up to 330V. The system interfaces with an off-chip, low power microcontroller (MCU) which provides a 100 kHz clock and four logic-level CMOS control signals. A digital state machine conditions the low-voltage signals for a high-voltage level shifter and gate-driver circuit, providing needed deadtime, high-current switching activation, and low-current state-holding modes. Only *one off-chip component* is needed – a 10nF COG MLCC capacitor which decouples the HV supply during switching.

Shown in Fig. 2, solar cells are trench-isolated and stacked in series and parallel domains to provide several voltage rails. A high-voltage (HV) array uses 196 series connected cells to provide 120-140V at optical density of 1-5 mW/mm<sup>2</sup>. A second array is used to power an off-chip MCU at  $\sim 1.8\text{V}$  and a third powers the I/O bus and on-chip digital control at  $\sim 3.6\text{V}$ .

Fig. 3 shows the HV level shift and drive circuit, state machine timing diagram, and oscilloscope screen shot of a single channel operating with the optical supply. The drive circuit uses 330V quasi-vertical DMOS devices in a complementary (class-B) configuration. The level shift circuit uses a low power 2-state current DAC to drive a floating 'accordion' OTA, referenced to the system high voltage (VDDH). When a switching transition is initiated, a high-current pulse sinks through HV

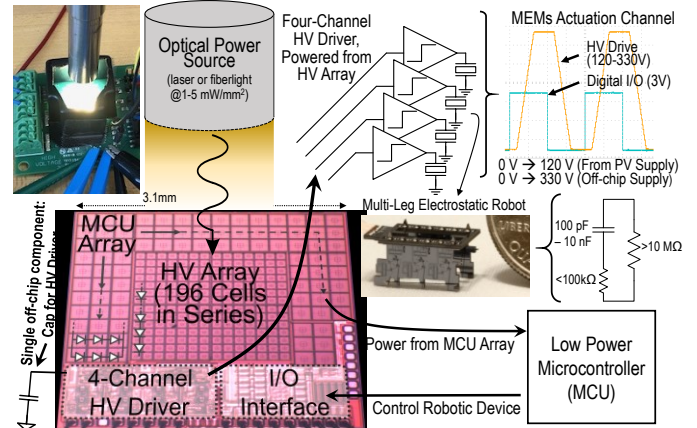


Fig. 1 System overview and block diagram.

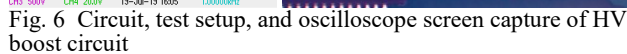
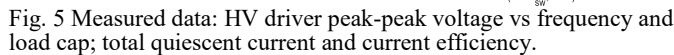
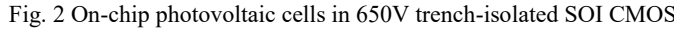
DMOS cascode devices into differential diode-connected NMOS-PMOS pair at  $V_{on,N/P}$  or  $V_{off,N/P}$ . The high current switching state remains for 5 clock cycles, then a low-current (90nA) state holding mode stays on for the duration of the switching state. Switching transitions are synchronized with a state machine including a 1-cycle ( $\sim 10\mu\text{s}$ ) deadtime between turn off/on of the complementary powertrain devices. A leakage clamp prevents residual sub-nA leakage in the DMOS cascodes from causing overvoltage stress on low voltage circuitry.

Fig 4 illustrates the operation of the floating accordion OTA which drives the HV-referenced PMOS device. When  $V_{on,N/P}$  are pulled down, M1 turns on, pulling up the gate of M3/4; this charges floating nodes  $V_{off,N/P}$ , turning M2 off and allowing  $P_{gate}$  to pull down through M4 (turning the HVP MOS 'on'). When  $V_{off,N/P}$  are pulled down, M3 and M2 turn on, pulling  $P_{gate}$  up and ensuring that M4 is off. Cross-coupling of the diode connected signals in the accordion OTA merges the gain of the PMOS differential pair and the NMOS current mirror, increasing gain, slew rate, and rise/fall time. This eliminates the use of any floating references, regulators, or latching structures, resulting in minimal quiescent power consumption other than the low-current state holding modes.

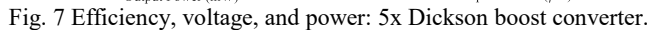
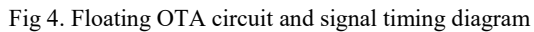
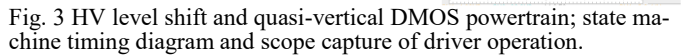
## Measurement Results

The chip was tested on a PCB platform that allowed operation *either* untethered (optical power to on-chip PV arrays) *or* with a single off-chip HV supply (used to measure quiescent current, current efficiency, and the peak voltage range of the drive circuit). Shown in Fig. 5, with a 1mW/mm<sup>2</sup> optical power source, the circuit could achieve 125V<sub>pp</sub> driving capacitive loads (40pF to 1nF), used to model the input reactance of typical actuators. Drive frequency of 10-100's of Hz was achieved, limited by the available power of the PV arrays and required reactive power of capacitive loads at given frequency and voltage. An off-chip power supply was used to characterize the power consumption of the system. Since the actuator driver is *hard-switching*, it incurs loss of  $C_{load}I_{drive}^2f_{sw}$  when driving reactive loads. Thus, like a linear regulator, we used current efficiency (*current delivered to load over current drawn from VDDH*) as a proxy for power utilization. With less than 1 $\mu\text{A}$  of

Shown in Fig. 6, the system was also tested as a switching power stage for a HV boost DC-DC converter; two HV driver channels were configured to drive the inputs of a differential Dickson voltage multiplier, [3]. Here, the drive circuits switch the reactive impedance of a network of flying capacitors (COG) with increasing voltage rating up to 1.5kV; SMT HV diodes rectify the drive signal, providing a 5x multiplied DC voltage output. Total board area was 0.7 cm<sup>2</sup>. Fig. 7 shows measured data for the boost converter, powered directly from a ~310V external voltage supply. The converter powertrain operated at ~1kHz to actuate the voltage multiplication stage,



Highlighted in Table I, this work is the first with optically powered high-voltage driving for MEMs-compatible voltages above 100V without custom post-processing steps. The PV array efficiency is the highest reported, due to the modular interconnect that increases the spatial efficiency compared to [4]. While overall system efficiency is lower compared to [5], which used a charge-recycling scheme, this work uses only *one off-chip component*, achieves higher driving voltages, and self-powered I/O and MCU control. **References:** [1] M. Karpelson, VLSI, 2011. [2] C. Bellew, TRANSDUCERS, 2003. [3] M. Forouzesh, TPEL, 2017. [4] Y. Hung, JEDS, 2017. [5] Y. Li, CICC, 2020



	[2] Bellow 03	[4] Hung 17	[5] Li 20	This Work
Process	Custom SOI	0.18 CMOS (cust. post-proc.)	650V SOI CMOS	650V SOI CMOS
V <sub>PP</sub> (SC,max)	100 V	12.5 V	88 V (16x5.5 V)	125 V
Area Solar	32 mm <sup>2</sup>	4 mm <sup>2</sup>	6 mm <sup>2</sup>	3 mm <sup>2</sup>
Irradiation	0.76 mW/mm <sup>2</sup>	6 mW/mm <sup>2</sup>	1-5 mW/mm <sup>2</sup>	1 mW/mm <sup>2</sup>
P (PV,out)	2010 $\mu$ W	125 $\mu$ W	Not reported	348 $\mu$ W
Efficiency	8.3 %	0.5%		11.5%
LV Supply	4.5 V	No HV driver	7.4 V	3.6 V
HV Output	48 V (PV)		88/118 V (PV/ext)	125/310 V (PV/ext)
DC Gain	10.7 (20.6 dB)		16 (24.0 dB)	86.1 (38.7 dB)
# Off-Chip Components	Not reported		16×0402 Capacitors	1×0603 Capacitor